


Visual Mnemonics in Neurovascular Imaging: A Gallery of Classic Ra-diological Signs

Ying Jie Toh*, Chi Long Ho, Louis Elliott McAdory

Department of Diagnostic Radiology, Sengkang General Hospital, Singapore

*Correspondence: Ying Jie Toh, Department of Diagnostic Radiology, Sengkang General Hospital, 110 Sengkang East Way, Singa-pore 544886

 tohyingjie@gmail.com

Radiology Case. 2025 August; 19(8):1-17 :: DOI: 10.3941/jrcr.5761

AUTHORS' CONTRIBUTIONS

Ying Jie Toh was involved in the original manuscript preparation and data collection.

Chi Long Ho and Louis Elliott McAdory were involved in the conceptualization of the study design, review and revision of the final manuscript.

ACKNOWLEDGEMENTS

None

DISCLOSURES

The authors do not have any conflict of interest, financial or non-financial disclosures.

CONSENT

Yes

HUMAN AND ANIMAL RIGHTS

Not applicable.

ABSTRACT

This pictorial review highlights key radiological signs integral to diagnosing neurovascular conditions. By pre-senting a curated collection of imaging examples, it emphasizes the characteristic features of various conditions observed on computed tomography (CT) and magnetic resonance imaging (MRI) of the brain and spinal cord. Inspired by familiar imagery from everyday life, these signs function as educational tools and memory aids, en-hancing medical professionals' ability to recognize and understand cerebrovascular pathologies, including devel-opmental, ischemic, hemorrhagic, and neoplastic processes. This gallery of signs aims to deepen awareness of neurovascular imaging and support radiologists in achieving accurate and timely diagnoses in clinical practice.

CASE REPORT

BACKGROUND

Metaphorical imaging signs provide intuitive visual cues that aid in the recognition of complex neurovascular conditions on CT and MRI. This pictorial review compiles 14 classic signs across developmental, ischemic, hemorrhagic, and neoplastic pathologies, offering a structured, image-based reference for radiologists. While many of these signs are well known individually, they have not previously been curated in a single, thematic reference tailored to neurovascular pathology. This article therefore serves as both an educational resource and a diagnostic guide, particularly valuable for trainees and clinicians involved in neuroimaging interpretation.

INTRODUCTION

Metaphorical imaging signs are widely described in radiology literature to illustrate the distinctive appearances of various neurovascular conditions, serving as essential tools for accurate

diagnosis. Inspired by familiar imagery such as animals, food, symbols, and objects, these signs function as intuitive aids, helping radiologists recall and interpret characteristic features across different imaging modalities.

This pictorial review presents 14 classic signs in neurovascular imaging, using case examples, images, and schematic illustrations. It highlights the key features of each sign and their associated diagnoses, supported by CT and MRI scans of the brain and spine from patients admitted to Sengkang General Hospital, Singapore, between 1 January 2016 and 1 November 2020.

The imaging signs are categorized by etiology as follows:

Developmental: Bag of worms, Black butterfly, Caput medusae, Kissing carotids, Popcorn, Tau

Ischemic: Cord, Empty delta, Hyperdense MCA, Puff of smoke, String of pearls, White cerebellum

Hemorrhagic: Spot, Zebra

Neoplastic: Salt and pepper

This collection provides radiologists with valuable educational tools for understanding and diagnosing a wide spectrum of neurovascular pathologies (Table 1).

CASE DESCRIPTION

Developmental conditions

Bag of worms sign

This sign describes the appearance of arteriovenous malformations (AVMs) which are high-flow vascular malformations characterized by direct arteriovenous shunting without an intervening capillary bed. It is composed of a nidus of vessels with multiple, tortuous and engorged feeding arteries and draining veins in a tangle of vessels resembling a bag of worms due to their convoluted and disorganized arrangement [1]. An AVM exhibits arterial enhancement and early venous drainage following contrast administration with the conventional cerebral angiography being gold standard of diagnosis due to rapid rate of shunting. The risk of intracranial hemorrhage from AVM is high with debilitating consequences. Treatment options include surgical resection, vascular embolization or radiosurgery [2]. Among the key considerations in AVM evaluation is surgical risk stratification, for which the Spetzler-Martin grading scale remains the most widely adopted tool [3] (Figures 1,2).

This grading system assesses three critical parameters that influence the operative risk associated with AVM resection, providing a framework for guiding microsurgical resection:

Parameter	Description	Points
Size of the AVM nidus	<3 cm (small), 3–6 cm (medium), >6 cm (large)	1, 2, 3
Eloquence of adjacent brain	Involvement of functionally critical areas (e.g., motor cortex, language centers, visual pathways)	0 (non-eloquent), 1 (eloquent)
Venous drainage pattern	Superficial only or deep venous drainage	0 (superficial), 1 (deep)

Grade I (1 point): Small, non-eloquent, superficial drainage

Grade II (2 points): Typically small or medium-sized with one risk factor

Grade III (3 points): Intermediate in complexity

Grade IV–V (4–5 points): Large, eloquent, and/or deep drainage — higher surgical risk

Grade VI: Occasionally used to denote lesions considered inoperable

Black butterfly sign

This sign describes symmetrical low signal intensity lesions predominantly in the dorsal aspect of the medulla and central gray matter of the cervical spinal cord on MRI T2*-weighted or susceptibility-weighted images (SWI). Resembling a black butterfly silhouette, this is suggestive of a dural arteriovenous fistula (DAVF) with spinal perimedullary venous drainage. Low

signal lesions on T2*-weighted and SWI are presumed selective hemorrhages partially caused by prolonged venous congestion and in gray matter with predilection for vulnerability to ischemia [4]. DAVFs can cause progressive myelopathy. Identifying this sign can facilitate the diagnosis of DAVF, differentiating DAVF from other spinal cord diseases such as demyelinating lesions and neoplasms. Treatment may include endovascular or surgical occlusion of the shunt (Figure 3).

Caput medusae sign

This sign is suggestive of a developmental venous anomaly (DVA), a congenital malformation of veins that drain the normal brain. Multiple anomalous dilated medullary venous tributaries arranged in a radial fashion drain into a larger vein, reminiscent of the appearance of Medusa's head from Greek mythology [5]. As a non-pathologic variation of venous drainage, DVA is usually clinically insignificant and an incidental finding. DVA carry a low annual hemorrhage risk, estimated at 0.15 to 0.34%, though this risk is significantly increased when associated with cavernomas [6] (Figure 4).

Kissing carotids sign

This sign describes a variant of the carotid arteries which are tortuous, elongated and abnormally close together or touch in the midline. The incidence of carotid arterial medialization is 12.3% with a severe aberrancy rate of 2.6% [7]. They can be located in the retropharyngeal, intrasphenoidal, or intrasellar regions, sometimes masquerading sellar or retropharyngeal pathology [8]. Awareness of this variant may help surgeons avoid these vessels during pharyngeal procedures like tonsillectomy and endoscopic transsphenoidal pituitary surgeries thereby reducing the risk of bleeding (Figures 5,6).

Popcorn sign

This sign describes the characteristic MRI appearance of cavernous venous malformations, commonly known as 'cavernous hemangiomas' or 'cavernomas', though they are now officially termed slow flow venous malformations according to newer International Society for the Study of Vascular Anomalies (ISSVA) nomenclature. They resemble a popcorn-like appearance with a T2-weighted hypointense rim and blooming on SWI due to susceptibility artefact from hemosiderin deposition. The signal characteristics vary depending the age of blood products contained [9] (Figure 7). Cavernous malformations can be classified into 4 types based on MRI appearances using the Zabramski classification [10]:

Type	Description	MRI Characteristics	Clinical Notes
Type I	Subacute hemorrhage	Hyperintense on T1-weighted and T2-weighted images (methemoglobin)	Recent bleed; may be symptomatic
Type II	Classic "popcorn" lesion	Mixed signal core with hypointense hemosiderin rim on T2-weighted images	Most common type; may show repeated hemorrhage

Type	Description	MRI Characteristics	Clinical Notes
Type III	Chronic resolved hemorrhage	Hypointense on T2-weighted images due to hemosiderin; no central core	Old, calcified; often asymptomatic
Type IV	Tiny, punctate microhemorrhages	Iso- or hypointense on SWI; not seen on conventional MRI	Often familial; may be multiple

Whilst most cavernous malformations are asymptomatic and can be treated conservatively, some can bleed and cause seizures or and may be treated with surgical resection.

Tau sign

The tau sign describes the appearance of a persistent primitive trigeminal artery (PPTA) on sagittal plane of CT or MRI angiography, resembling the Greek letter “τ” [11]. PPTA is one of the persistent carotid-vertebrobasilar anastomoses and is prevalent in 0.1-0.6% of the general population and usually presents unilaterally. In fetal development, the trigeminal artery supplies the primitive vertebrobasilar system prior to the formation of the posterior communicating and vertebral arteries. Most PPTAs arise from the junction between petrous and cavernous internal carotid artery, and runs posterolaterally along the trigeminal nerve or crosses over or through the dorsum sellae with nearly equal frequency (Figure 8).

Saltzman classification categorizes PPTAs into two main types with other combination of these variants [12]. In Saltzman type I configuration, the PPTA supplies the cranial basilar artery including the posterior cerebral artery territories, entering between the superior cerebellar arteries and the anterior inferior cerebellar arteries. The posterior communicating artery, caudal basilar artery and distal vertebral arteries are either absent or hypoplastic. In Saltzman type II configuration, the PPTA supplies the superior cerebellar arteries. It is usually associated with fetal origins of the posterior cerebral arteries. Identifying this vascular anomaly is important when performing neurovascular interventions to avoid non-target embolization.

Ischemic conditions

Cord sign and Empty delta sign

The cord sign is suggestive of dural venous sinus thrombosis (DVST) typically seen along the transverse sinus on unenhanced CT, where an elongated cord-like hyperattenuation is seen along the venous sinus on axial scans [13]. Caution should be exercised to avoid overcalling the findings, as normal blood within the venous sinuses can appear slightly hyperdense compared to the brain parenchyma on unenhanced CT (Figure 9).

The empty delta sign is suggestive of DVST typically seen along the superior sagittal sinus on contrast-enhanced CT venography as well as MR venography, where the contrast outlines a triangular filling-defect caused by the non-enhancing thrombus resembling the Greek letter 'Δ'. Despite being a reliable sign, it is seen only in 25-30% of DVST cases. This

sign may not be seen in the early stage of thrombosis (<5 days), as the fresh clot is hyperdense, or in the late stage (>2 months) where numerous recanalization channels may have developed within the thrombus [14].

Timely recognition of these signs can facilitate early diagnosis and the prompt initiation of anticoagulant therapy.

Hyperdense MCA sign and insular ribbon sign

Dense artery sign was first described by Gyula Gács, a renowned Hungarian neurologist-psychiatrist in 1983, referred to as "Gács sign". The hyperdense MCA sign refers to focal hyperdensity of the middle cerebral artery (MCA) on unenhanced CT which indicates intraluminal thromboembolus and occlusion of the MCA due to relative increased density compared to the brain parenchyma of the offending clot [15], with Hounsfield units (HU) greater than 43 and ratio to contralateral MCA greater than 1.2 [16]. It is the one of the earliest imaging sign of MCA infarction [17] and is highly specific (up to 90%) [18], along with "insular ribbon sign" which refers to the loss of gray-white differentiation of the insular cortex [19] (Figure 10).

Puff of smoke sign or Moyamoya appearance

The term Moyamoya meaning "puff of smoke" in Japanese, describes the appearance of dense, network-like pattern of tiny, fragile collateral vessels that resemble smoke on cerebral angiography [20]. This sign is associated with progressive stenosis of the anterior circulation and supraclinoid internal carotid arteries, leading to the development of extensive collateral circulation originating from the lenticulostriate and choroidal arteries (Figure 11).

When the cause of the occlusion is unknown, it is referred to as Moyamoya disease. In contrast, Moyamoya syndrome occurs as a result of a variety of secondary conditions including atherosclerosis, vasculitic/inflammatory causes, infection, radiation therapy and blood dyscrasias [21]. The disease is commonly linked with cerebral ischemia or infarction in children, and hemorrhage in adults [22].

Diagnosis is confirmed through angiography, and treatment typically involves strategies to manage the vascular abnormalities, such as surgical revascularization or bypass procedures. The Suzuki angiographic staging system is used to describe the progression of Moyamoya disease and classifies the disease into six stages based on digital subtraction angiography findings:

Stage	Angiographic Features	Key Changes	Collateral Formation
Stage I	Narrowing of distal internal carotid artery (ICA)	Initial ICA stenosis	No prominent collaterals yet
Stage II	Initiation of Moyamoya vessels	ICA stenosis progresses	"Puff of smoke" collaterals begin forming from lenticulostriate arteries

Stage	Angiographic Features	Key Changes	Collateral Formation
Stage III	Intensification of Moyamoya vessels	Collaterals become dense	Peak collateral formation; classic “Moyamoya” appearance
Stage IV	Minimization of Moyamoya vessels	Main arteries further narrowed	Collaterals start regressing; new extracranial–intracranial pathways begin
Stage V	Reduction of Moyamoya vessels	ICA may be nearly occluded	External carotid artery (ECA) collaterals increase
Stage VI	Disappearance of Moyamoya vessels	ICA fully occluded	Brain perfused mainly by ECA and vertebrobasilar system collaterals

String of pearls appearance

This appearance describes watershed infarcts on MRI which occur at the cortical and deep border zones between cerebral vascular territories [23]. It is characterized by the presence of multiple, small foci of restricted diffusion. These lesions are arranged in a somewhat linear fashion parallel to the lateral ventricles in the watershed areas [24], for example in the centrum semiovale or corona radiata between the penetrating cortical arteries and ascending perforating arteries (internal watershed zone) as well as at the borders of vascular territories (external watershed zone) of the brain [25] (Figure 12).

These watershed infarctions account for approximately 10% of ischemic strokes and are often caused by a combination of cerebral hypoperfusion and microemboli, with a higher incidence in the elderly [26].

White cerebellum sign or reversal sign

This sign describes a diffuse hypodensity of the cerebral hemispheres, with loss of gray-white differentiation and a relative hyperdensity of the thalami, brainstem and cerebellum on CT [27]. It represents anoxic/ischemic cerebral injury and indicates irreversible brain damage. It may be seen in hypoxic ischemic encephalopathy, severe head injury, birth asphyxia, drowning, status epilepticus, bacterial meningitis and encephalitis. Approximately one-third of patients with this sign die, while the remaining survivors may experience significant long-term neurological impairments [28] (Figure 13, 14).

One proposed mechanism explaining the appearance is distension of the deep medullary veins secondary to partial obstruction of venous outflow due to raised intracranial pressure. Other theories include preferential flow to the posterior circulation and transtentorial herniation partially relieving the raised intracranial pressure, leading to improved perfusion of structures like the brainstem [29]. While the imaging pattern of hypoxic ischemic encephalopathy is variable in pattern in adults, a pattern of increased symmetric restricted diffusion with T2-weighted or Fluid attenuated inversion recovery (FLAIR) signal abnormality can occur in the brain regions including diffuse cortical involvement including or sparing the perirolandic cortex, deep grey matter and cerebellum.

Hemorrhagic conditions

Angiographic positive spot sign

This sign is defined as small single focal area of contrast enhancement within an acute primary intraparenchymal hemorrhage on dynamic CT angiography [30]. It corresponds to a site of active hemorrhage and is an independent predictor of intracerebral hematoma growth and portends poor clinical outcome [31]. The reverse is also true, meaning that the lack of a spot sign indicates that the hematoma is unlikely to grow substantially in size [32] (Figure 15).

Zebra sign (cerebellum)

This sign describes the CT appearance of blood layering the cerebellar folia with hyperdense cerebellar sulcal blood alternating with isodense brain, giving a streaky pattern resembling zebra’s stripes [33]. It is seen in the setting of supratentorial or neurovascular surgeries possibly secondary to dural tear typically within the first 72 hours [34], deemed as remote cerebellar hemorrhage away from the site of surgery with often benign clinical outcome [35] (Figure 16).

Neoplastic condition

Salt and pepper sign

This sign aptly summarizes the classic MRI appearance and features of a paraganglioma, an uncommon, highly vascular neuroendocrine tumor. It describes the mass's speckled pattern, where the "salt" represents areas of high intrinsic T1 signal from slow-flowing blood or hemorrhages, and the "pepper" denotes multiple vascular flow voids caused by the prominent vessels typical of these hypervascular tumors, which also show avid contrast enhancement [36]. Paragangliomas in the head and neck are commonly found in locations such as the carotid body, jugular foramen, along the vagus nerve, and the middle ear [37] (Figure 17).

Whilst this sign is highly sensitive for localizing tumors, it lacks specificity in definitively distinguishing a paraganglioma from other hypervascular masses. Functional imaging with various tracer options serves as a valuable adjunct for diagnosing and staging paragangliomas. Treatment options may involve surgical removal or radiation therapy.

CONCLUSION

This pictorial review highlights the significance of key imaging signs in diagnosing a diverse range of neurovascular conditions. By emphasizing the characteristic features of developmental anomalies, ischemic, hemorrhagic, and neoplastic pathologies, these signs serve as invaluable tools for radiologists to achieve rapid and accurate diagnoses. Drawing inspiration from familiar imagery, these signs function as both educational aids and cognitive anchors, simplifying the interpretation of complex imaging findings. By enhancing diagnostic efficiency and guiding timely, targeted treatments,

this curated collection of imaging signs may contribute to better patient management. It also serves as a valuable resource for radiologists and trainees, fostering a deeper understanding and recognition of the neurovascular spectrum in clinical practice.

TEACHING POINT

This pictorial review presents 14 classic metaphorical imaging signs that distill complex neurovascular pathology into easily recognizable visual patterns inspired by familiar imagery. Categorized by etiology into developmental, ischemic, hemorrhagic, and neoplastic pathologies and supported by case examples and schematic illustrations, the review offers a practical learning framework to support radiologists and trainees in accurately identifying and recalling the characteristic features of neurovascular lesions on CT and MRI scans, thereby enhancing diagnostic precision and clinical decision-making.

QUESTIONS

Question 1: Which of the following statements regarding the bag of worms sign is correct?

1. It describes the imaging appearance of a cavernous venous malformation.
2. It is composed of a nidus of vessels with tortuous and engorged feeding arteries and draining veins. (applies)
3. It is best diagnosed using ultrasound.
4. The risk of intracranial hemorrhage is low.
5. Surgical resection is the only treatment option.

Explanation:

1. The bag of worms sign describes an arteriovenous malformations (AVMs). [This sign describes the appearance of arteriovenous malformations (AVMs) which are high-flow vascular malformations characterized by direct arteriovenous shunting without an intervening capillary bed.]
2. It is composed of a nidus of vessels with tortuous and engorged feeding arteries and draining veins. [It is composed of a nidus of vessels with multiple, tortuous and engorged feeding arteries and draining veins in a tangle of vessels resembling a bag of worms due to their convoluted and disorganized arrangement.]
3. Conventional cerebral angiography is the gold standard for diagnosis, not ultrasound. [An AVM exhibits arterial enhancement and early venous drainage following contrast administration with the conventional cerebral angiography being gold standard of diagnosis due to rapid rate of shunting.]
4. The risk of intracranial hemorrhage from AVMs is high, not low [The risk of intracranial hemorrhage from AVM is high with debilitating consequences.]
5. Treatment options are not only limited to surgical resection but also less invasive techniques like vascular embolization or radiosurgery. [Treatment options include surgical resection, vascular embolization or radiosurgery.]

Question 2: What is the Caput Medusae sign associated with?

1. Arteriovenous malformations (AVMs).
2. A pathologic variation of venous drainage requiring urgent treatment.
3. Progressive myelopathy.
4. Developmental venous anomaly (DVA). (applies)
5. High risk of spontaneous hemorrhage.

Explanation:

1. The Caput Medusae sign is suggestive of a developmental venous anomaly (DVA), instead of an AVM. [This sign is suggestive of a developmental venous anomaly (DVA), a congenital malformation of veins that drain the normal brain. Multiple anomalous dilated medullary venous tributaries arranged in a radial fashion drain into a larger vein, reminiscent of the appearance of Medusa's head from Greek mythology.]
2. A DVA is a non-pathologic variation of venous drainage and is usually an incidental finding with no clinical significance. [As a non-pathologic variation of venous drainage, DVA is usually clinically insignificant and an incidental finding.]
3. It is not associated with progressive myelopathy—this is more typical of DAVFs [DAVFs can cause progressive myelopathy.]
4. The Caput Medusae sign describes the typical appearance of a DVA. [This sign is suggestive of a developmental venous anomaly (DVA), a congenital malformation of veins that drain the normal brain. Multiple anomalous dilated medullary venous tributaries arranged in a radial fashion drain into a larger vein, reminiscent of the appearance of Medusa's head from Greek mythology.]
5. While DVAs can be associated with cavernomas, which may lead to hemorrhagic complications, DVA itself does not indicate a high risk of spontaneous hemorrhage [DVA carry a low annual hemorrhage risk, estimated at 0.15 to 0.34%, though this risk is significantly increased when associated with cavernomas.]

Question 3: Which of the following statements regarding the hyperdense MCA sign is correct?

1. It is best seen on MRI.
2. It indicates an intraluminal thromboembolus in the middle cerebral artery. (applies)
3. It is a late imaging finding of ischemic stroke.
4. It has a low specificity for MCA infarction.
5. It was first described by Gyula Gács. (applies)

Explanation:

1. The hyperdense MCA sign is a CT finding, not an MRI finding. [The hyperdense MCA sign refers to focal hyperdensity of the middle cerebral artery (MCA) on unenhanced CT which indicates intraluminal thromboembolus and occlusion of the MCA due to relative increased density compared to the brain parenchyma of the offending clot, with Hounsfield units (HU) greater than 43 and ratio to contralateral MCA greater than 1.2.]
2. It indicates the presence of an intraluminal thromboembolus in the middle cerebral artery, leading to its occlusion. [The hyperdense MCA sign refers to focal hyperdensity of the middle

cerebral artery (MCA) on unenhanced CT which indicates intraluminal thromboembolus and occlusion of the MCA due to relative increased density compared to the brain parenchyma of the offending clot, with Hounsfield units (HU) greater than 43 and ratio to contralateral MCA greater than 1.2.]

3. It is one of the earliest imaging signs of MCA infarction, not a late finding. [It is the one of the earliest imaging sign of MCA infarction and is highly specific (up to 90%), along with "insular ribbon sign" which refers to the loss of gray-white differentiation of the insular cortex.]

4. It has high specificity (up to 90%) for MCA infarction. [It is the one of the earliest imaging sign of MCA infarction and is highly specific (up to 90%), along with "insular ribbon sign" which refers to the loss of gray-white differentiation of the insular cortex.]

5. The sign was first described by Gyula Gács in 1983, also known as the "Gács sign". [Dense artery sign was first described by Gyula Gács, a renowned Hungarian neurologist-psychiatrist in 1983, referred to as "Gács sign".]

Question 4: Which of the following are true of Moyamoya appearance?

1. It is associated with arteriovenous malformations.
2. It is associated with progressive stenosis of the anterior circulation and supraclinoid internal carotid arteries. (applies)
3. It is always due to a primary genetic disorder.
4. It refers to dense, network-like pattern of tiny, fragile collateral vessels. (applies)
5. It is best seen on non-contrast CT.

Explanation:

1. It is a description of network of tiny collateral vessels resembling smoke, characteristic for Moyamoya syndrome or Moyamoya disease, instead of AVMs which typically resemble a bag of worms with a nidus of vessels with multiple, tortuous and engorged feeding arteries and draining veins. [The term Moyamoya meaning "puff of smoke" in Japanese, describes the appearance of dense, net-work-like pattern of tiny, fragile collateral vessels that resemble smoke on cerebral angiography.]

2. The Moyamoya appearance describes the formation of prominent lenticulostriate and choroidal collaterals, associated with progressive stenosis of the anterior circulation and supraclinoid internal carotid arteries. [This sign is associated with progressive stenosis of the anterior circulation and supraclinoid internal carotid arteries, leading to the development of extensive collateral circulation originating from the lenticulostriate and choroidal arteries.]

3. It is not always due to a primary genetic disorder – Moyamoya disease is idiopathic, but Moyamoya syndrome can result from various secondary conditions such as atherosclerosis, vasculitis, infection, and radiation therapy. [When the cause of the occlusion is unknown, it is referred to as Moyamoya disease. In contrast, Moyamoya syndrome occurs as a result of a variety of secondary conditions including atherosclerosis, vasculitic/inflammatory causes, infection, radiation therapy and blood dyscrasias.]

4. It refers to dense, network-like pattern of tiny, fragile collateral vessels. [The term Moyamoya, meaning "puff of smoke" in Japanese, describes the appearance of dense, network-like pattern of tiny, fragile collateral vessels that resemble smoke on cerebral angiography.]

5. It is best appreciated on contrast-enhanced CT angiography or conventional cerebral angiography. [Diagnosis is confirmed through angiography, and treatment typically involves strategies to manage the vascular abnormalities, such as surgical revascularization or bypass procedures.]

Question 5: Which of the following imaging findings is most associated with dural venous sinus thrombosis (DVST)?

1. Salt and pepper sign
2. Empty delta sign (applies)
3. Zebra sign
4. String of pearl sign
5. Popcorn sign

Explanation:

1. Salt and pepper sign describes a paraganglioma on MRI rather than DVST. [This sign aptly summarizes the classic MRI appearance and features of a paraganglioma, an uncommon, highly vascular neuroendocrine tumor. It describes the mass's speckled pattern, where the "salt" represents areas of high intrinsic T1 signal from slow-flowing blood or hemorrhages, and the "pepper" denotes multiple vascular flow voids caused by the prominent vessels typical of these hypervascular tumors, which also show avid contrast enhancement.]

2. The empty delta sign, seen on contrast-enhanced CT venography, is a classic imaging finding in dural venous sinus thrombosis (DVST). [The empty delta sign is suggestive of DVST typically seen along the superior sagittal sinus on contrast-enhanced CT venography as well as MR venography, where the contrast outlines a triangular filling-defect caused by the non-enhancing thrombus resembling the Greek letter 'Δ'.]

3. Zebra sign suggests remote cerebellar hemorrhage away from the site of surgery on CT. [This sign describes the CT appearance of blood layering the cerebellar folia with hyperdense cerebellar sulcal blood alternating with isodense brain, giving a streaky pattern resembling zebra's stripes. It is seen in the setting of supratentorial or neurovascular surgeries possibly secondary to dural tear typically within the first 72 hours, deemed as remote cerebellar hemorrhage away from the site of surgery with largely benign clinical outcome.]

4. The string of pearls sign describes the presence of multiple watershed infarcts on MRI instead of DVST. [This appearance describes watershed infarcts on MRI which occur at the cortical and deep border zones between cerebral vascular territories]

5. Popcorn sign describes the characteristic MRI appearance of a cavernous venous malformations rather than DVST. [This sign describes the characteristic MRI appearance of cavernous venous malformations, commonly known as 'cavernous hemangiomas' or 'cavernomas', though they are now officially termed slow flow venous malformations according to newer International Society for the Study of Vascular Anomalies (ISSVA) nomenclature. They resemble a popcorn-like

appearance with a T2-weighted hypointense rim and blooming on SWI due to susceptibility artifact from hemosiderin deposition. The signal characteristics vary depending the age of blood products contained.]

REFERENCES

- Geibprasert S, Pongpech S, Jiarakongmun P, Shroff MM, Armstrong DC, Krings T. Radiologic assessment of brain arteriovenous malformations: what clinicians need to know. *Radiographics*. 2010; 30(2): 483-501. PMID: 20228330.
- Ajiboye N, Chalouhi N, Starke RM, Zanaty M, Bell R. Cerebral arteriovenous malformations: evaluation and management. *ScientificWorldJournal*. 2014; 2014: 649036. PMID: 25386610.
- Spetzler RF, Martin NA. A proposed grading system for arteriovenous malformations. *J Neurosurg*. 1986; 65(4): 476-483. PMID: 3760956.
- Enokizono M, Sato N, Morikawa M, et al. "Black butterfly" sign on T2*-weighted and susceptibility-weighted imaging: A novel finding of chronic venous congestion of the brain stem and spinal cord associated with dural arteriovenous fistulas. *J Neurol Sci*. 2017; 379: 64-68. PMID: 28716281.
- Saba PR. The caput medusae sign. *Radiology*. 1998; 207(3): 599-600. PMID: 9609879.
- Ku MG, Rhee DY, Park HS, Kim DN. Repeated intracerebral hemorrhage from developmental venous anomaly alone. *J Korean Neurosurg Soc*. 2009; 45(1): 46-49. PMID: 19242572.
- Koreckij J, Alvi H, Gibly R, Pang E, Hsu WK. Incidence and risk factors of the retropharyngeal carotid artery on cervical magnetic resonance imaging. *Spine (Phila Pa 1976)*. 2013; 38(2): E109- E112. PMID: 23124269.
- Pereira Filho Ade A, Gobbato PL, Pereira Filho Gde A, Silva SB, Kraemer JL. Intracranial intrasellar kissing carotid arteries: case report. *Arq Neuropsiquiatr*. 2007; 65(2A): 355-357. PMID: 17607445.
- Hegde AN, Mohan S, Lim CC. CNS cavernous haemangioma: "popcorn" in the brain and spinal cord. *Clin Radiol*. 2012; 67(4): 380-388. Nov 30. PMID: 22137800.
- Zabramski JM, Wascher TM, Spetzler RF, et al. The natural history of familial cavernous malformations: results of an ongoing study. *J Neurosurg*. 1994; 80(3): 422-432. PMID: 8113854.
- Goyal M. The tau sign. *Radiology*. 2001; 220(3): 618-619. PMID: 11526258.
- Saltzman GF. Patent primitive trigeminal artery studied by cerebral angiography. *Acta Radiol (Stockh)*. 1959; 51(5): 329-336. PMID: 13649384.
- Vijay RK. The cord sign. *Radiology*. 2006; 240(1): 299-300. PMID: 16793988.
- Lee EJ. The empty delta sign. *Radiology*. 2002; 224(3): 788-789. PMID: 12202715.
- Gács G, Fox AJ, Barnett HJ, Vinuela F. CT visualization of intracranial arterial thromboembolism. *Stroke*. 1983; 14(5): 756-762. PMID: 6658961.
- Koo CK, Teasdale E, Muir KW. What constitutes a true hyperdense middle cerebral artery sign? *Cerebrovasc Dis*. 2000; 10(6): 419-423. PMID: 11070370.
- Tomsick T, Brott T, Barsan W, et al. Prognostic value of the hyperdense middle cerebral artery sign and stroke scale score before ultraearly thrombolytic therapy. *AJNR Am J Neuroradiol*. 1996; 17(1): 79-85. PMID: 8770253.
- Jensen-Kondering U, Riedel C, Jansen O. Hyperdense artery sign on computed tomography in acute ischemic stroke. *World J Radiol*. 2010; 2(9): 354-357. PMID: 21160697.
- Truwit CL, Barkovich AJ, Gean-Marton A, Hibri N, Norman D. Loss of the insular ribbon: another early CT sign of acute middle cerebral artery infarction. *Radiology*. 1990; 176(3): 801-806. PMID: 2389039.
- Ortiz-Neira CL. The puff of smoke sign. *Radiology*. 2008; 247(3): 910-911. PMID: 18487544.
- Mossa-Basha M, Shibata DK, Hallam DK, et al. Added Value of Vessel Wall Magnetic Resonance Imaging for Differentiation of Nonocclusive Intracranial Vasculopathies. *Stroke*. 2017; 48(11): 3026-3033. PMID: 29030476.
- Suzuki J, Takaku A. Cerebrovascular "moyamoya" disease. Disease showing abnormal net-like vessels in base of brain. *Arch Neurol*. 1969; 20(3): 288-299. PMID: 5775283.
- Derdeyn CP, Khosla A, Videen TO, et al. Severe hemodynamic impairment and border zone--region infarction. *Radiology*. 2001; 220(1): 195-201. PMID: 11425997.
- Rotman J, Zimmerman R. Patterns of ischemic stroke: from lacunar to territorial to multiple embolic to watershed hypotensive. In: Saba L, Raz E, editors. *Neurovascular imaging*. New York (NY): Springer; 2014. p. 353-355.
- Dogariu OA, Dogariu I, Vasile CM, et al. Diagnosis and treatment of Watershed strokes: a narrative review. *J Med Life*. 2023; 16(6): 842-850. PMID: 37675172.
- Rovira A, Grivé E, Rovira A, Alvarez-Sabin J. Distribution territories and causative mechanisms of ischemic stroke. *Eur Radiol*. 2005; 15(3): 416-426. PMID: 15657788.
- Han BK, Towbin RB, De Courten-Myers G, McLaurin RL, Ball WS Jr. Reversal sign on CT: effect of anoxic/ischemic cerebral injury in children. *AJNR Am J Neuroradiol*. 1989; 10(6): 1191-1198. PMID: 2512781.
- Badejo OA, Nwafuluaku EC, Olatunji RB, Balogun JA. White cerebellum sign as a dark prognostic indicator of cerebral injury: A case report. *Ann Ib Postgrad Med*. 2024; 22(1): 108-111. PMID: 38939880.

29. Chavhan GB, Shroff MM. Twenty classic signs in neuroradiology: A pictorial essay. *Indian J Radiol Imaging*. 2009; 19(2): 135-145. PMID: 19881070.
30. Wada R, Aviv RI, Fox AJ, et al. CT angiography "spot sign" predicts hematoma expansion in acute intracerebral hemorrhage. *Stroke*. 2007; 38(4): 1257-1262. PMID: 17322083.
31. Demchuk AM, Dowlatshahi D, Rodriguez-Luna D, et al. Prediction of haematoma growth and outcome in patients with intracerebral haemorrhage using the CT-angiography spot sign (PREDICT): a prospective observational study. *Lancet Neurol*. 2012; 11(4): 307-314. PMID: 22405630.
32. Romero JM, Hito R, Dejam A, et al. Negative spot sign in primary intracerebral hemorrhage: potential impact in reducing imaging. *Emerg Radiol*. 2017; 24(1): 1-6. PMID: 27553777.
33. Brockmann MA, Nowak G, Reusche E, Russlies M, Petersen D. Zebra sign: cerebellar bleeding pattern characteristic of cerebrospinal fluid loss. Case report. *J Neurosurg*. 2005; 102(6): 1159-1162. PMID: 16028781.
34. Nagendran A, Patel B, Khan U. The zebra sign: an unknown known. *Pract Neurol*. 2016; 16(1): 48-49. PMID: 26271264.
35. Figueiredo EG, de Amorim RL, Teixeira MJ. Remote cerebellar hemorrhage (zebra sign) in vascular neurosurgery: pathophysiological insights. *Neurol Med Chir (Tokyo)*. 2009; 49(6): 229-233. PMID: 19556730.
36. Olsen WL, Dillon WP, Kelly WM, Norman D, Brant-Zawadzki M, Newton TH. MR imaging of paragangliomas. *AJR Am J Roentgenol*. 1987; 148(1): 201-204. PMID: 3024473.
37. Rao AB, Koeller KK, Adair CF. Paragangliomas of the head and neck: radiologic-pathologic correlation. Armed Forces Institute of Pathology. *Radiographics*. 1999; 19(6): 1605-1632. PMID: 10555678.

FIGURES

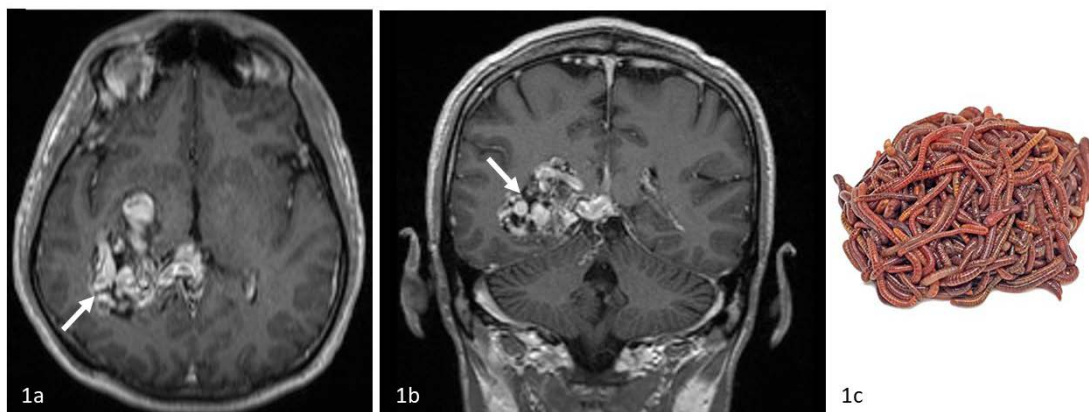


Figure 1: Bag of worms sign. 54 year old male with large cerebral arteriovenous malformation. Axial (1a) and coronal (1b) contrast-enhanced T1-weighted MR images showing multiple serpiginous flow voids of feeding arteries and draining veins, resembling a “bag of worms” in the right medial temporal and hippocampal regions. This is compatible with a large arteriovenous malformation with the nidus centered in the right temporal and hippocampal regions (white arrows) with associated arterial aneurysms and venous varix partly extending into the temporal horn of the right lateral ventricle. Siemens Avanto, 1.5 Tesla, T1-weighted coronal MPRAGE, Slice width 1.0 mm, TR 1300, TE 4.32, FA 15, Intravenous contrast: 10 ml Dotarem. (1c) Image of a bag of worms.

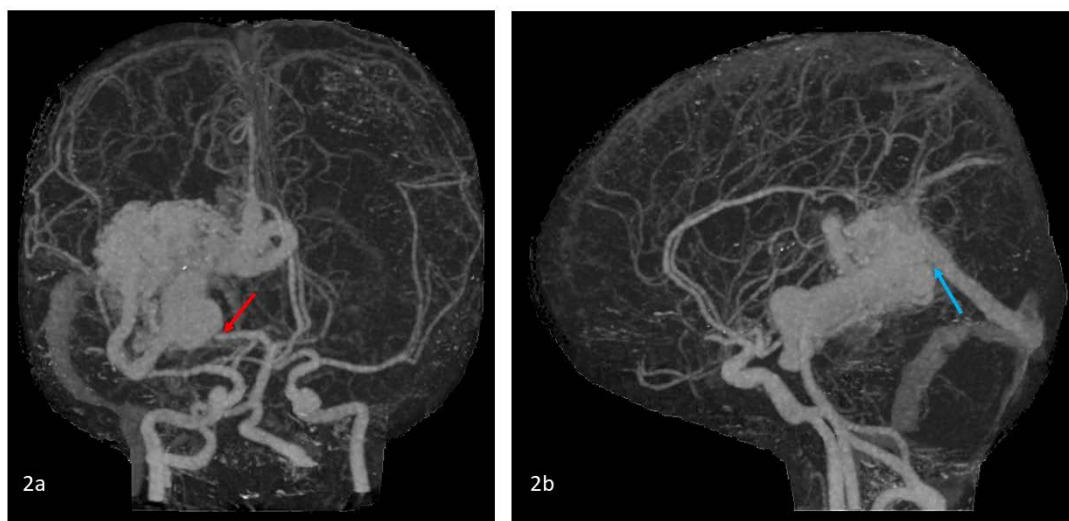


Figure 2: Bag of worms sign. 54 year old male with large cerebral arteriovenous malformation. CT angiography of the Circle of Willis 3D volume-rendered reconstruction shows that the arteriovenous malformation is primarily supplied by the right posterior cerebral artery (PCA) (red arrow in 2a) and drains via the vein of Galen and straight sinus (blue arrow in 2b). Toshiba Aquilion One, Slice width 3.0 mm, 120 kV, 114 mAs, Intravenous contrast: 60 ml Omnipaque

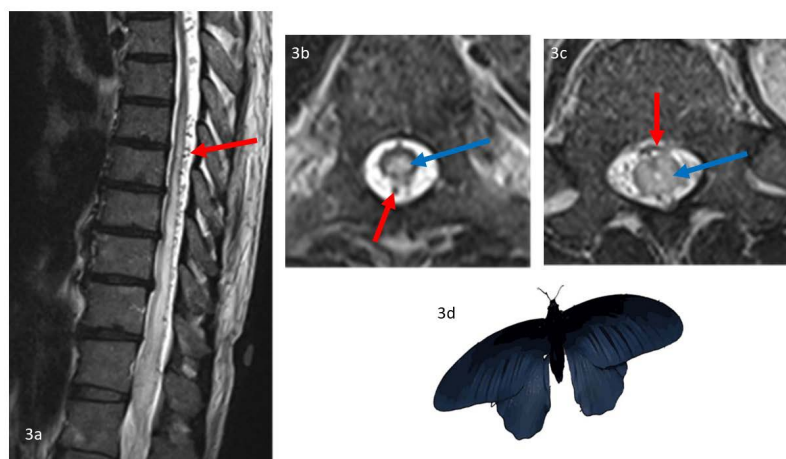


Figure 3: Black butterfly sign. 22 year old male with cord edema secondary to thoracic spinal dural arteriovenous fistula (DAVF). (3a) Sagittal T2-weighted spinal MRI showing a swollen lower thoracic spinal cord with central hyperintensity surrounded by tortuous, serpentine and dilated perimedullary venous plexus with flow voids (red arrow). Axial T2-weighted images at T8 (3b) and T12 (3c) levels show T2-weighted hyperintensity of the cord (blue arrows) surrounded by engorged perimedullary venous plexus with flow voids (red arrows). Siemens Aera, 1.5 Tesla, Slice width 3.0 mm, TR 4000, TE 86, FA 150. (3d) An image of a black butterfly.

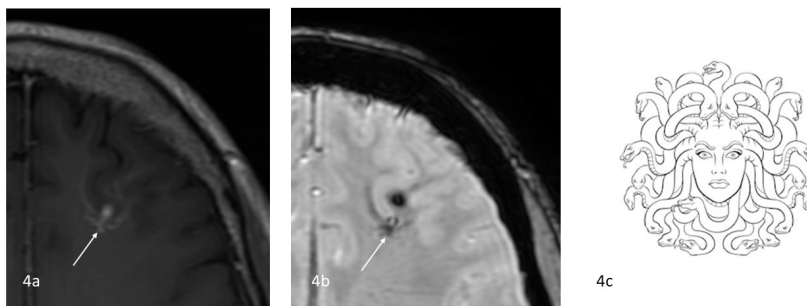


Figure 4: Caput medusae sign. 63 year old female with cerebral developmental venous anomaly (DVA). Axial (4a) contrast-enhanced T1-weighted and (4b) susceptibility-weighted MR images reveal a faintly enhancing lesion in the left frontal lobe with associated blooming susceptibility artefact, seemingly arranged in a radial fashion draining into a larger vein (thin white arrow). The appearance resembles Medusa's head, referred to as the "caput medusae sign", indicating a cerebral DVA. GE Medical Systems Signa Architect, 3.0 Tesla, Slice width 4.0 mm, TR 550, TE 8.19 FA 111 for T1-weighted fast spin echo (FSE) with contrast and Slice width 2.0 mm, TR 43.6, TE 24.1, FA 10 for 3D susceptibility-weighted angiography (SWAN), Intravenous contrast: 10 ml Dotarem. (4c) Caput medusa or Medusa's head (Medusa is a gorgon of Greek mythology).

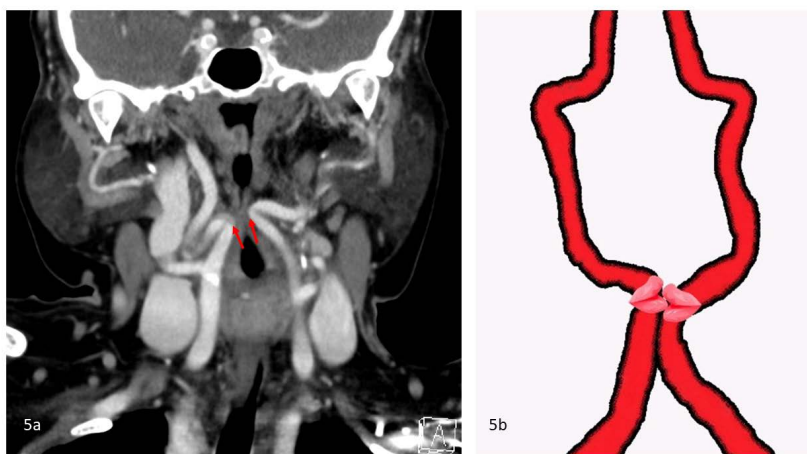


Figure 5: Kissing carotids sign. 77 year old female with retropharyngeal course of bilateral internal carotid arteries. (5a) Contrast-enhanced CT neck coronal reformats demonstrates tortuous and elongated internal carotid arteries (red arrows) with medial deviation and approximating in the midline in their prevertebral course, suggestive of retropharyngeal "kissing carotids". Siemens Somatom Definition Flash, Slice width 3.0 mm, 100kV, 176 mAs, Intravenous contrast: 60ml Omnipaque 350. (5b) Cartoon illustration of retropharyngeal "kissing carotids".

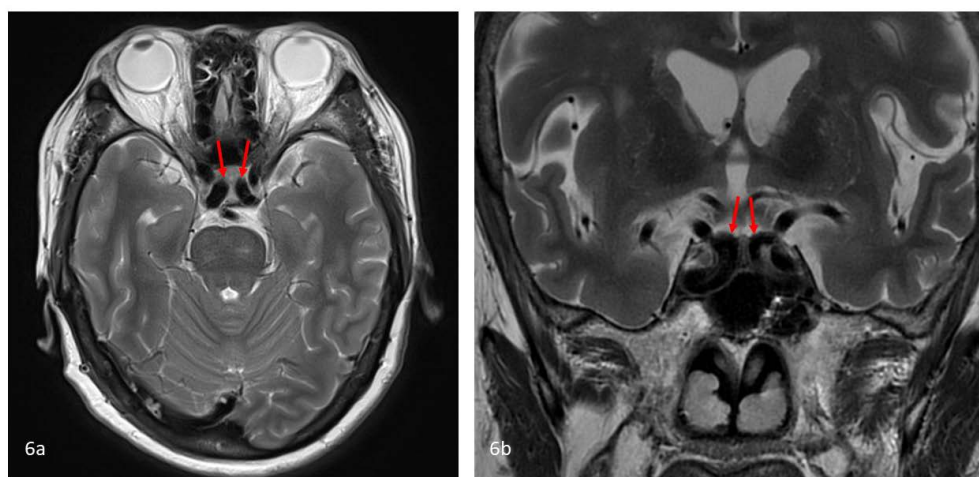


Figure 6: Kissing carotids sign. 75 year old female with bilateral tortuous cavernous internal carotid arteries. Axial (6a) and coronal (6b) T2-weighted MR images of the brain showing tortuous bilateral cavernous carotid arteries which deviated into the sella approximating each other (red arrows), suggestive of intra-sellar “kissing carotids”. Axial: Siemens Magnetom Skyra, 3.0 Tesla, Slice width 4.0 mm T2-weighted sequence, TR 5460 TE 92 FA 90; Coronal: Siemens Magnetom Aera, 1.5 Tesla, Slice width 2.5 mm, T2-weighted sequence, TR 2950 TE 112 FA 150.

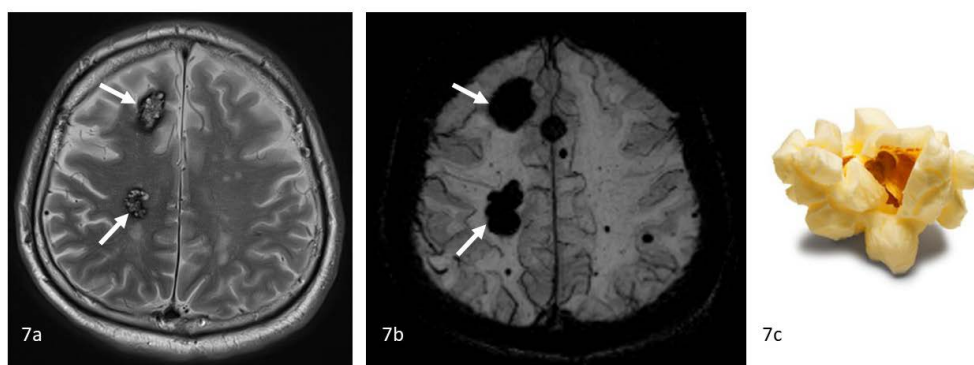


Figure 7: Popcorn sign. 65 year old male with multiple cerebral cavernous malformations. Multiple cavernous malformations (white arrows) in the right cerebral hemisphere showing (7a) popcorn-like appearance with a hypointense rim on T2-weighted imaging and (7b) blooming artifact on susceptibility-weighted imaging (SWI) due to hemosiderin deposition. Innumerable microhemorrhages are also seen scattered throughout both cerebral hemispheres. (7c) Image of a popcorn. Siemens Magnetom Skyra, 3.0 Tesla, T2-weighted sequence: Slice width 4.0 mm, TR 4000 TE 92 FA 90; SWI MIP sequence: Slice width 16.0 mm TR 27 TE 20 FA 15.

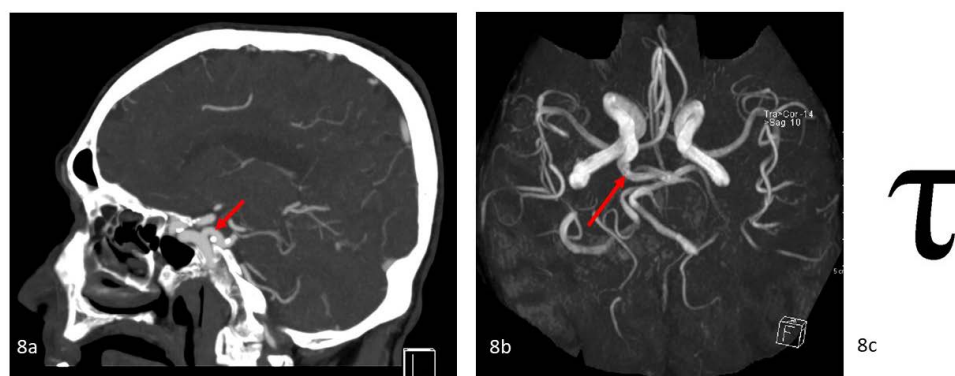


Figure 8: Tau sign. 73 year old male with right persistent primitive trigeminal artery. (8a) CT angiography of the Circle of Willis sagittal reformats show a persistent trigeminal artery (red arrow), forming the Greek letter ‘τ’ (tau). Siemens Somatom Force, 80 kV, 239mAs, Intravenous contrast: 60 ml Omnipaque 350. (8b) Time of flight MR angiography 3D volume-rendered reconstruction of the Circle of Willis shows a large-calibre artery (red arrow) arising from the ICA and joining the basilar artery tip, consistent with right persistent primitive trigeminal artery Saltzman type I. Siemens Aera, 1.5 Tesla, TR 24 TE 7 FA 25. (8c) Greek letter ‘τ’ or tau.

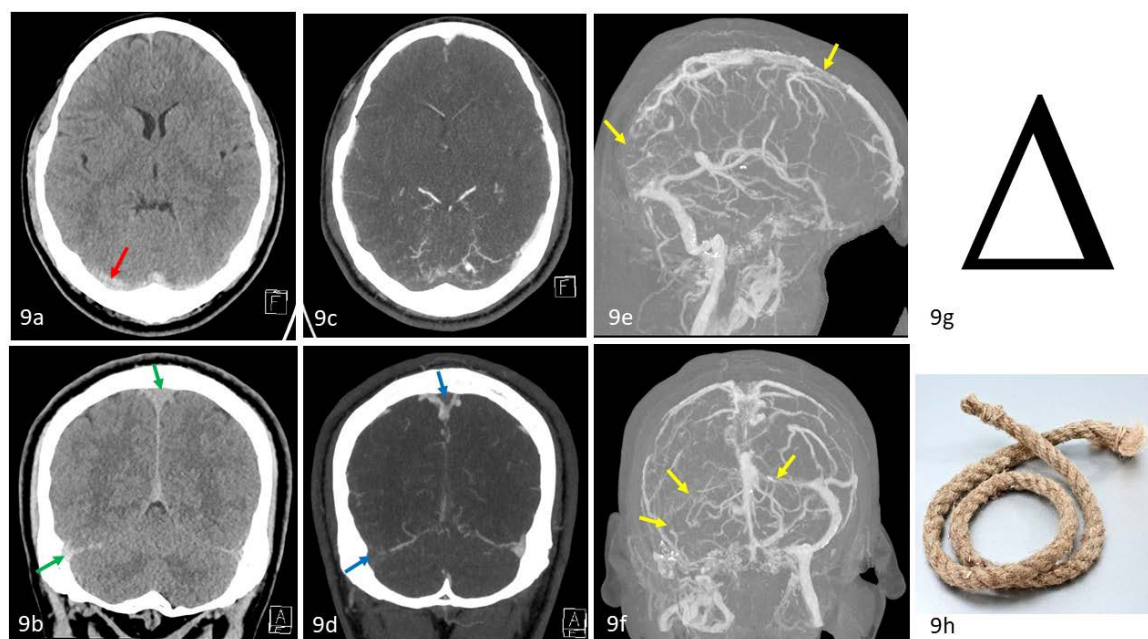


Figure 9: Cord sign and Empty delta sign. 36 year old male with dural venous sinus thrombosis. (9a) Axial unenhanced CT shows cord-like hyperattenuation seen along the right transverse sinus (red arrow) suggestive of the "cord sign" for dural venous sinus thrombosis. (9b) Coronal unenhanced CT shows hyperdense superior sagittal and right transverse sinuses (green arrows). (9c, 9d) Axial and coronal CT venogram shows central filling defects outlined by contrast in the superior sagittal sinus and right transverse sinus (blue arrows) demonstrating the "empty delta sign". (9e, 9f) CT venogram 3D volume-rendered reconstruction shows non-opacification of the posterior two-third of the superior sagittal sinus, proximal left and complete right transverse sinuses and right sigmoid sinus (yellow arrows). These are compatible with dural venous sinus thrombosis. Unenhanced CT: Siemens Somatom Force, Slice width 3.0 mm, 120 kV, 296 mAs; CT venogram: Siemens Somatom Force, Slice width 3.0 mm, 80 kV, 97 mAs, Intravenous contrast: 60 ml Omnipaque 350. (9g) Greek letter 'Δ' or delta. (9h) Image of a cord/rope.

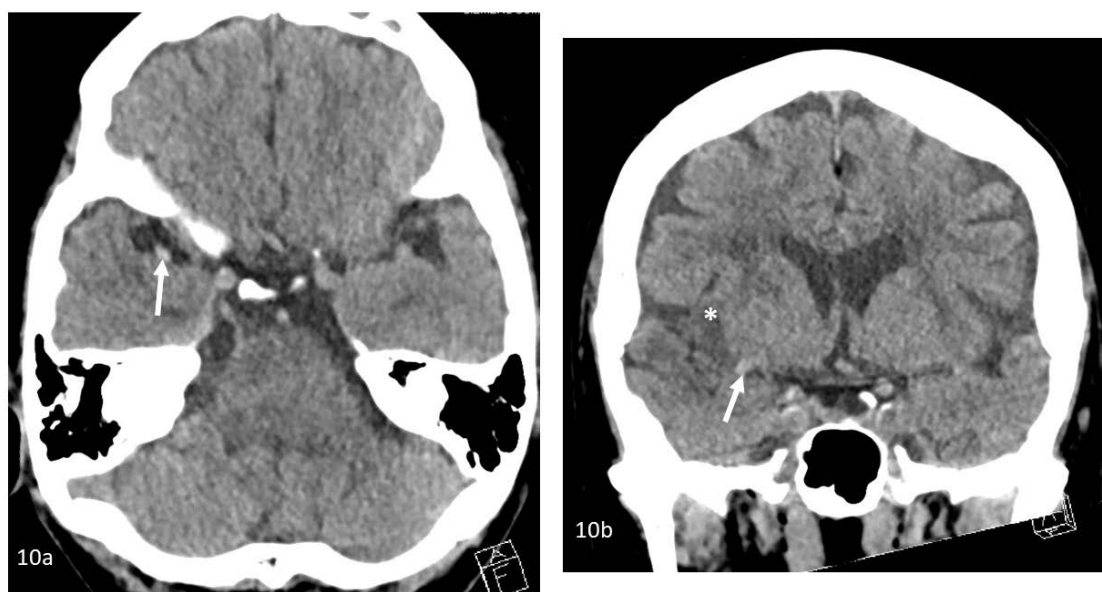


Figure 10: Hyperdense MCA sign and loss of insular ribbon sign. 72 year old female with acute right MCA infarct. Axial (10a) and coronal (10b) unenhanced CT brain shows a hyperdense right MCA (white arrow) which is due to the offending thromboembolus in the right MCA. There is also loss of gray-white differentiation and edema at the right insular cortex (white asterisk) which is referred as the "loss of insular ribbon sign", suggestive of an acute right MCA infarct. Toshiba Aquilion Prime, Slice width 3.0 mm, 120 kV, 150 mAs

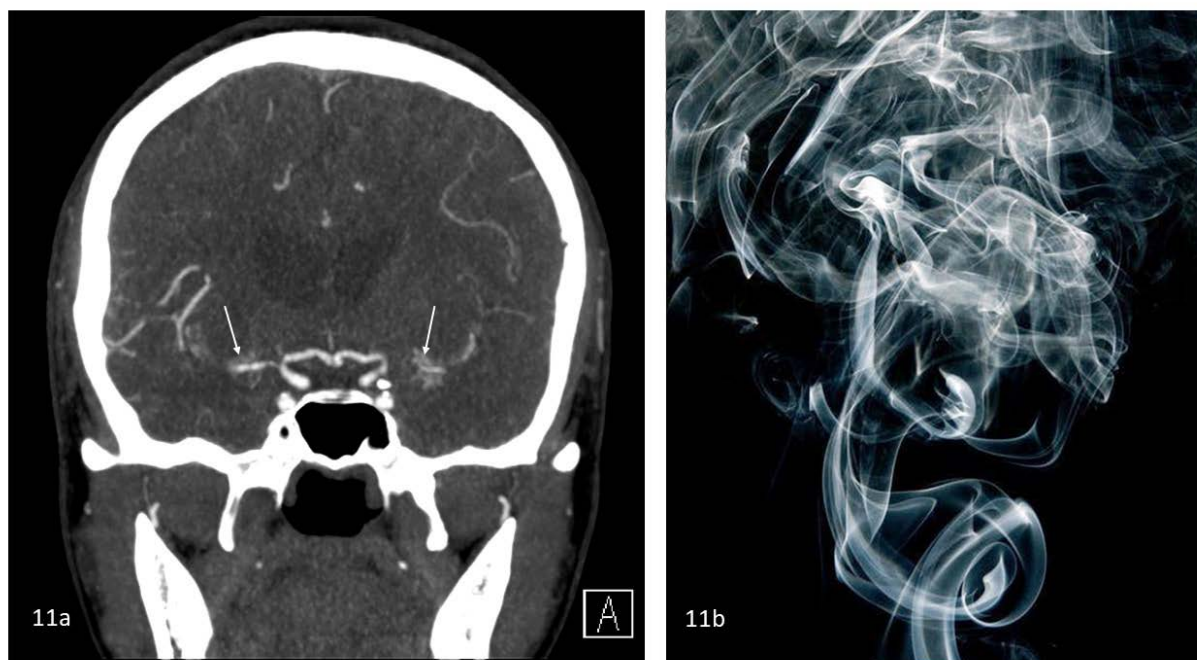


Figure 11: Puff of smoke sign or Moyamoya appearance. 47 year old male with Moyamoya disease or variant. (11a) Coronal maximum intensity projection (MIP) reformats of the CT angiography of the Circle of Willis shows narrowing at the bilateral carotid terminus and M1 segments of the bilateral MCAs with multiple small collateral vessels (thin white arrows) reminiscent of the Moyamoya (puff of smoke) appearance. Siemens Somatom Force, Slice width 5.0 mm, 80 kV, 211 mAs, Intravenous contrast: 55 ml Omnipaque 350. (11b) Illustration of puff of smoke.

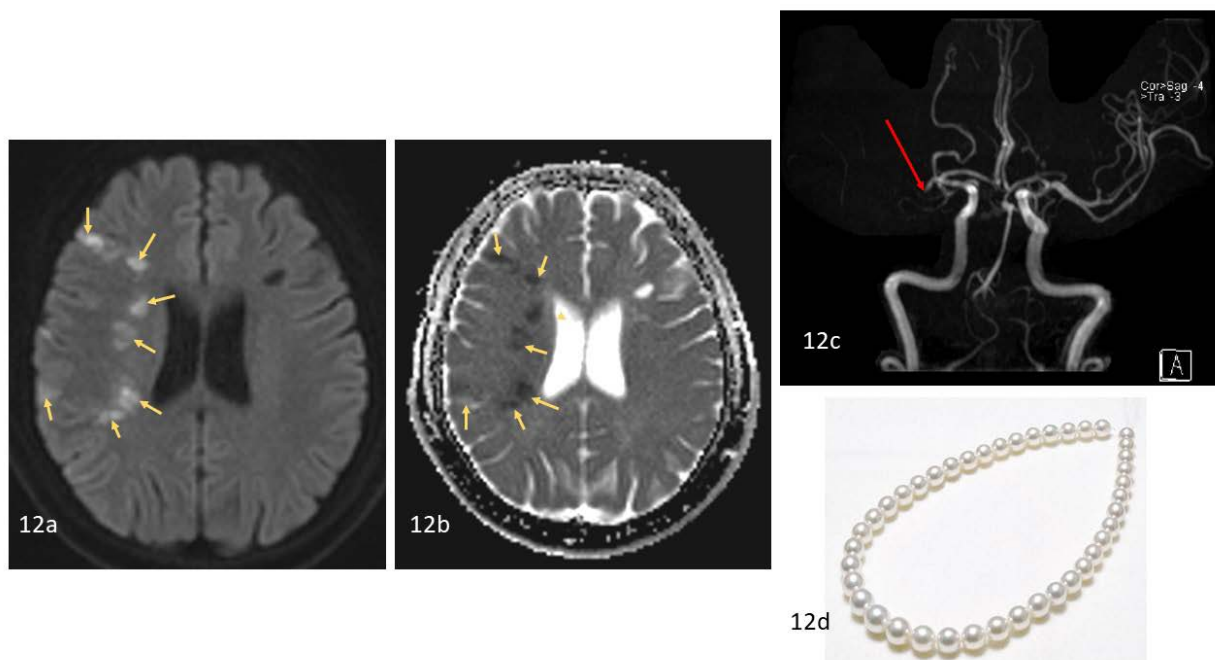


Figure 12: Strings of pearls sign. 48 year old female with acute watershed infarcts in the right MCA territory. Multiple foci of restricted diffusion, appearing bright on DWI (12a) and dark on ADC (12b) are seen in the right frontal and right temporal lobes as well as in the right corona radiata (yellow arrows) in the internal and cortical border zones between the right MCA and right ACA and PCA, resembling a string of pearls. This is suggestive of acute watershed infarcts in the right MCA territory. (12c) Time of Flight MR angiography of the Circle of Willis 3D volume-rendered reconstruction shows abrupt cut-off at the proximal right M1 segment (red arrow), likely due to an occlusive thrombus. Siemens Aera, 1.5 Tesla, Slice width 5.0 mm, TR 5040, TE 52, FA 180. (12d) String of pearls imagery.

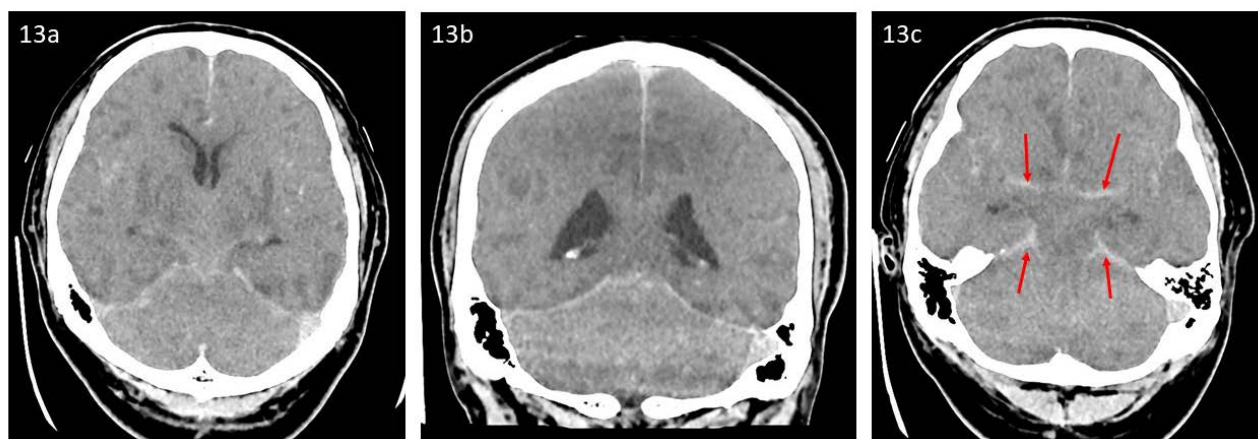


Figure 13: White cerebellum sign or reversal sign. 33 year old male with hypoxic ischemic encephalopathy (HIE). Axial (13a) and coronal (13b) unenhanced CT brain shows low attenuation of the cerebral hemispheres with complete loss of gray matter–white matter differentiation and effacement of the basal cisterns, suggestive of massive cerebral edema. There is relative hyperattenuation of the cerebellum compared to the supratentorial brain giving the appearance of “white cerebellum sign”. The constellation of findings are compatible with HIE. (13c) Apparent symmetrical hyperdensities (red arrows) confined to the basal cisterns are likely due to a combination of cisternal effacement, distension of vessels and relative contrast difference with the adjacent brain suggestive of “pseudo-subarachnoid hemorrhage” sign seen in HIE. GE Medical Systems Revolution CT, Slice width 3.0 mm, 140 kV, 1mAs.

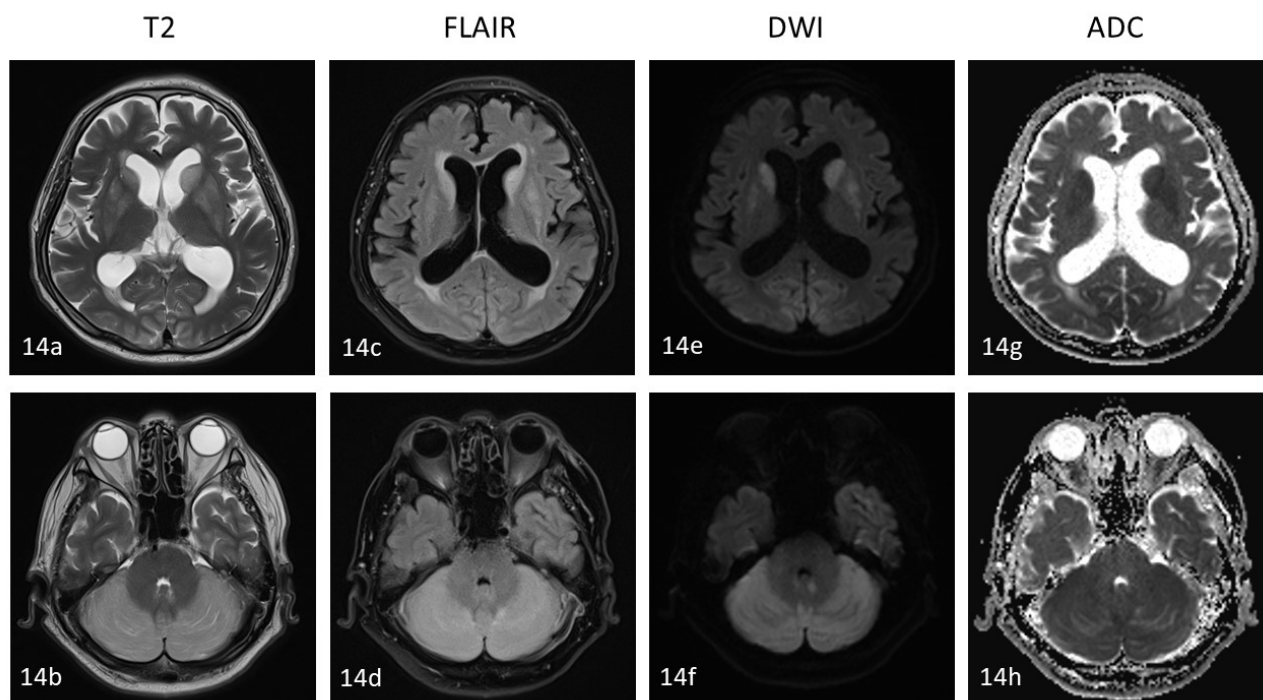


Figure 14: White cerebellum sign or reversal sign. 66 year old male with HIE. Axial imaging of supratentorial brain (14a, 14b, 14c, 14d) and infratentorial brain (14e, 14f, 14g, 14h) in T2-weighted, FLAIR, DWI and ADC sequences from left to right respectively. There are scattered areas of restricted diffusion with associated FLAIR and T2-weighted signal seen in the bilateral cerebellar hemispheres and also in the deep grey matter notably in the bilateral caudate and lentiform nuclei symmetrically. Associated mass effect with compression of the fourth ventricle and associated dilatation of the third and lateral ventricles in keeping with hydrocephalus. Findings are in keeping with underlying HIE. Siemens Aera, 1.5 Tesla, 5 mm slice T2-weighted sequence: TR 5200, TE 104, FA 121; FLAIR sequence: TR 6000 TE 98 FA 150; DWI/ADC sequences: TR 5040 TE 62 FA 180.

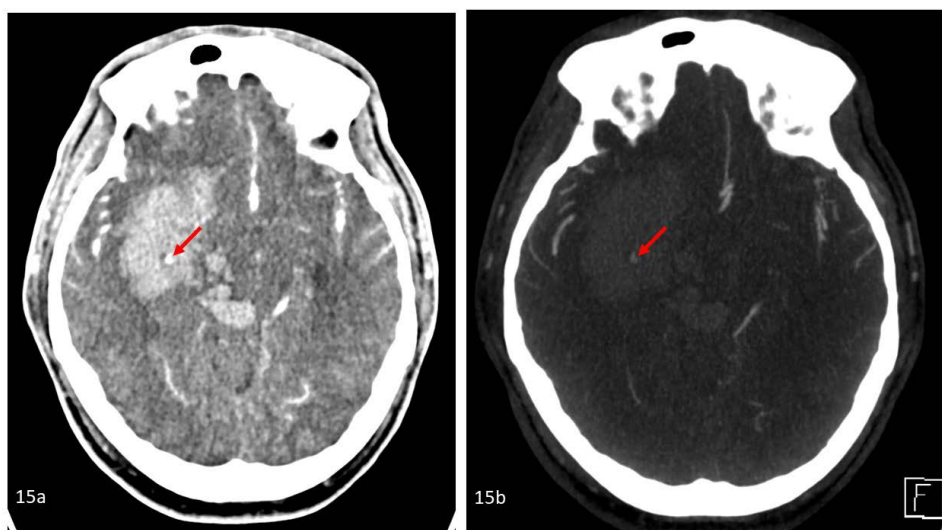


Figure 15: Angiographic positive spot sign. 39 year old male with large intraparenchymal hematoma with signs of active bleed. (15a) CT angiogram of the Circle of Willis with (15b) maximum intensity projection (MIP) show a large acute intraparenchymal hematoma centered in the right basal ganglia and thalamus with intraventricular extension. A subcentimeter area of contrast enhancement within the hematoma is suggestive of a positive angiographic “spot sign” (red arrows), concerning for active hemorrhage. Siemens Somatom Force, Slice width 3.0 mm, 80 kV, 206 mAs; Intravenous contrast: 60 ml Omnipaque 350.

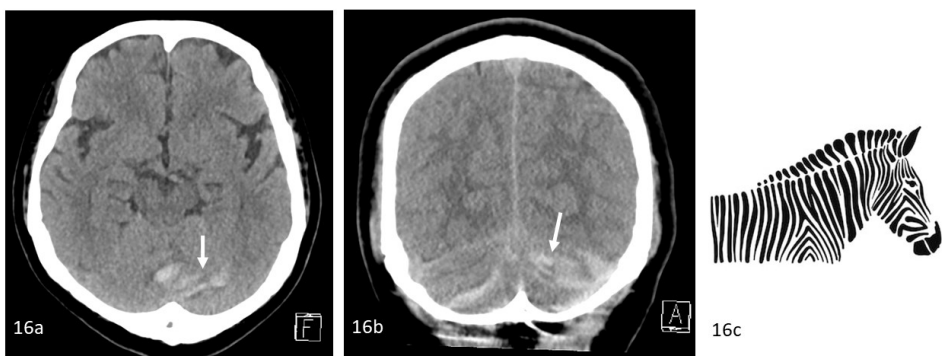


Figure 16: Zebra sign. 56 year old female with remote cerebellar hemorrhage post supratentorial craniotomy for clipping of paraclinoid aneurysm. Axial (16a) and coronal (16b) unenhanced CT brain demonstrating layering of blood amongst the folia of the cerebellum (white arrows) suggestive of remote cerebellar hemorrhage. Siemens Somatom Force, Slice width 3 mm, 120 kV, 245 mAs. (16c) Schematic illustration of a zebra.

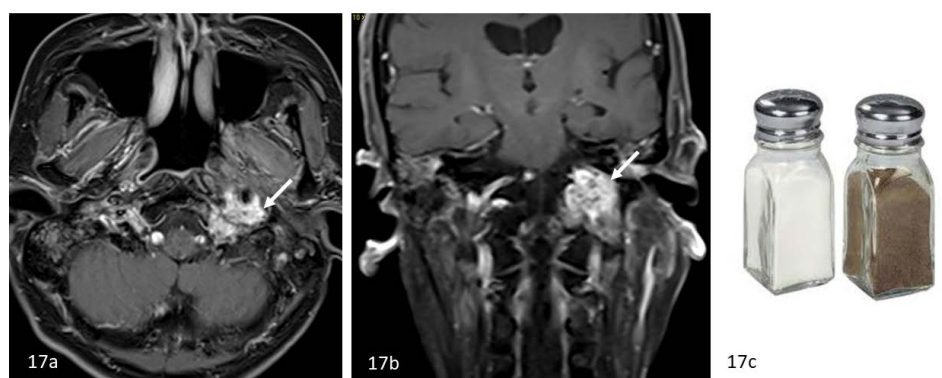


Figure 17: Salt and pepper sign. 62 year old male with a jugular paraganglioma. Axial (17a) and coronal (17b) contrast enhanced T1-weighted images shows an avidly enhancing mass with characteristic salt-and-pepper speckled appearance in the left jugular foramen with multiple areas of signal voids (white arrows), suggestive of a jugular paraganglioma. There is adjacent bony erosion and encasement of the left internal carotid artery. (17c) Image of table salt and pepper. Siemens Aera (1.5 Tesla, Slice width 5.0 mm, Axial: TR 625 TE 11 FA 146, Coronal: TR 691 TE 8.6 FA 150. Intravenous contrast: 10 ml Dotarem.

Table 1: Imaging Signs

Category	Imaging Sign	Description	Diagnosis
Developmental	Bag of worms	Tangled, tortuous vessels comprising a nidus and engorged cerebral arterial supply and venous drainage	Arteriovenous malformation (AVM)
	Black butterfly	T2-weighted hyperintensity within the cord surrounded by engorged perimedullary venous plexus with flow voids	Dural arteriovenous fistula (DAVF)
	Caput medusae	Radial arrangement of dilated medullary venous tributaries draining into subependymal or cerebral veins	Developmental venous anomaly (DVA)
	Kissing carotids	Tortuous, medially displaced ICAs approximate each other in the midline, typically in the retropharyngeal or intrasellar regions	Carotid artery variant
	Popcorn	T2-weighted hypointense rim and blooming on SWI due to hemosiderin deposition, and variable internal signal intensity reflecting blood products of different ages	Cavernous venous malformation
	Tau	Persistent carotid-basilar anastomosis resembling Greek letter “τ” on sagittal CT/MRI angiography	Persistent primitive trigeminal artery (PPTA)
Ischemic	Cord and Empty delta	Cord-like hyperdensity along the dural venous sinus, with the triangular filling defect seen on CT or MR venography	Dural venous sinus thrombosis (DVST)
	Hyperdense MCA	Focal hyperdensity in the MCA representing occlusive thromboembolus (>43 HU)	Middle cerebral artery (MCA) infarction
	Puff of smoke	Dense network of collateral lenticulostriate and choroidal arteries on angiography with stenosis of the supraclinoid ICAs.	Moyamoya disease/syndrome
	String of pearls	Small foci of restricted diffusion in a linear fashion at vascular border zones	Watershed infarcts
	White cerebellum	Diffuse cerebral hypodensity with relative hyperdensity of the brainstem and cerebellum on CT	Anoxic/ischemic brain injury
Hemorrhagic	Angiographic spot	Focal contrast enhancement within acute intracerebral hematoma on dynamic CT angiography	Active intracerebral hemorrhage
	Zebra cerebellum	Hyperdense blood within the cerebellar folia alternating with isodense cerebellar tissue on CT	Remote cerebellar hemorrhage
Neoplastic	Salt and pepper	Speckled MRI pattern due to high intrinsic T1 signal and vascular flow voids with avid enhancement	Paraganglioma

KEYWORDS

Neurovascular imaging, Radiological signs, Computed tomography (CT), Magnetic resonance imaging (MRI), Cerebrovascular pathology, Developmental anomalies, Ischemic stroke, Hemorrhagic stroke, Neoplastic conditions, Diagnostic radiology

ABBREVIATIONS

ADC = APPARENT DIFFUSION COEFFICIENT
 AVM = ARTERIOVENOUS MALFORMATION
 CT = COMPUTED TOMOGRAPHY
 CTA = COMPUTED TOMOGRAPHY ANGIOGRAPHY
 DAVF = DURAL ARTERIOVENOUS FISTULA
 DWI = DIFFUSION-WEIGHTED IMAGING
 DVA = DEVELOPMENTAL VENOUS ANOMALY
 DVST = DURAL VENOUS SINUS THROMBOSIS
 ECA = EXTERNAL CAROTID ARTERY
 FA = FLIP ANGLE
 FLAIR = FLUID ATTENUATED INVERSION RECOVERY
 FSE = FAST SPIN ECHO
 HIE = HYPOXIC ISCHEMIC ENCEPHALOPATHY
 HU = HOUNSFIELD UNITS
 ICA = INTERNAL CAROTID ARTERY
 ISSVA = INTERNATIONAL SOCIETY FOR THE STUDY OF VASCULAR ANOMALIES
 MCA = MIDDLE CEREBRAL ARTERY
 MIP = MAXIMUM INTENSITY PROJECTION
 MPRAGE = MAGNETIZATION-PREPARED RAPID GRADIENT ECHO
 MRI = MAGNETIC RESONANCE IMAGING
 PCA = POSTERIOR CEREBRAL ARTERY
 PPTA = PERSISTENT PRIMITIVE TRIGEMINAL ARTERY
 SWAN = SUSCEPTIBILITY-WEIGHTED ANGIOGRAPHY
 SWI = SUSCEPTIBILITY-WEIGHTED IMAGING
 TE = TIME TO ECHO
 TR = TIME TO REPETITION

Online access

This publication is online available at:
www.radiologycases.com/index.php/radiologycases/article/view/5761

Peer discussion

Discuss this manuscript in our protected discussion forum at:
www.radiopolis.com/forums/JRCR

Interactivity

This publication is available as an interactive article with scroll, window/level, magnify and more features.
 Available online at www.RadiologyCases.com

Published by EduRad



www.EduRad.org